

Special Issue: “Selected Papers from 12th International Conference of the Hellenic Geographical Society (ICHGS): Innovative Geographies II, 2019”

Modification of a groundwater prospect zone index using remotely sensed data and the analytic network process in the eastern part of Lesvos island, Greece.

Terpsichori K. MITSI^{1*}, Demetre P. ARGIALAS¹,
Konstantinos VAMVOUKAKIS¹

¹ National and Technical
University of Athens, Greece

Keywords:

Remote Sensing,
groundwater,
remote sensing data,
MGPI,
Analytic Network
Process

Abstract

Because of climate change and overpopulation, the demand for water is increasing. Groundwater constitutes an alternative renewable source of aquifer, so the spatial distribution of ground water provides important information on its qualitative and quantitative status. This paper develops a methodology for delineating potential ground water zones using remotely sensed data and GIS. The developed methodology was based on the empirical index GPI (MGPI – Modified Groundwater Potential Index) and was applied to the eastern part of Lesvos Island, Greece. To evaluate the criteria used for the result, the Analytic Network Process (ANP) was applied to weight each parameter. The dataset used consists of satellite images derived from Sentinel 2 and Landsat 8, which were combined with vector and raster data, to create the necessary thematic layers. To validate the results, existing ground water zones from the Municipal Water Company of Lesvos were used.



© Association of European
Geographers

The publication of the European Journal of Geography (EJG) is based on the European Association of Geographers' goal to make European Geography a worldwide reference and standard. Thus, the scope of the EJG is to publish original and innovative papers that will substantially improve, in a theoretical, conceptual or empirical way the quality of research, learning, teaching and applying geography, as well as in promoting the significance of geography as a discipline. Submissions are encouraged to have a European dimension. The European Journal of Geography is a peer-reviewed open access journal and is published quarterly.

1. INTRODUCTION

Groundwater is part of the hydrological cycle and goes into and out of the deepest layers of the soil (Papanikolaou & Sideris, 2013). The presence of groundwater in an area depends on several factors such as the porosity of the soil, the permeability of the rocks, the climate and seismic activity. The ability of a soil to "store" water in its resources is called *permeability to water* or *water permeability* and depends on the different shapes, sizes and arrangement of the granule in it. Locating and exploiting groundwater resources is a multi-dimensional issue, which is particularly important as the demand for water increases due to the population growth and the intense urbanization (Abdala, 2012). Therefore, groundwater could be characterized as an alternative renewable water resource.

The identification and utilization of groundwater resources requires the combination of different disciplines and tools. One of those disciplines is remote sensing. Through remote sensing, it is possible to assess in which areas potential groundwater zones are located at a minimum cost and less time than a measurement in the field. Most of the remotely sensed images are free of charge and ready to be downloaded in different formats. In this paper, images used are derived from Sentinel 2 and Landsat 8 satellites and they are already calibrated to Bottom of Atmosphere Reflectance (BoA) format, which provides an estimate of the surface reflectance as it would be measured in the absence of atmospheric effects.

The study area is the eastern part of the island of Lesvos, which includes the capital of the island, Mytilene, the peninsula of Amali, the gulf of Çera, the region of Plomari and the mountain of Olympus, including Agiassos. The island was divided into the eastern, central and western part taking into consideration the geological background of each region. The western part is covered by volcanic rock, the central part by metamorphic, and the east by limestone. The rocks of eastern Lesvos are pre-alpine and Alpine of the Neo-Paleozoic and Triad centuries (Katsikatsos et al, 1982). The region is also called an "indigenous zone", because of the marine and lake sediments that prevail in it (Katsikatsos et al. 1982, Mountrakis, 2010). In the area, limestone, sandstone, rattlesnake and clay can be found, also marble and carbonic rocks. The porous and loose structure of limestone rock allows water to pass through the soil resources, so it is appropriate to identify possible additional areas of groundwater in this area.

2. BACKGROUND

2.1 Literature review

The aim of this paper was the development of a methodology for the detection of groundwater using remote-sensing data and Geographic Information Systems (GIS). In recent years, remote sensing and GIS have been widely used for groundwater studies with the aim of minimizing field measurements (Solomon & Quiel, 2006; Krishnamurthy et al, 2010; Abdalla 2012; Partsineveloy et al, 2012).

Krishnamurthy et al. (2000) describes the modification and adjustment of the empirical indices, GPI or GWPI (Ground Water Potential Index) or GWP (Ground Water

Prospect). The index was based on overlapping weighted levels (multicriterial analysis). GPI was referred to as the GIS model for the detection of groundwater supply. The model receives 10 input data, lithology, landforms, land use, soil characteristics, drainage density, saturation zone thickness and fracture zone, wells, other aquatic bodies and lineaments. The layers are not weighted but are combined with each other and their average is the result.

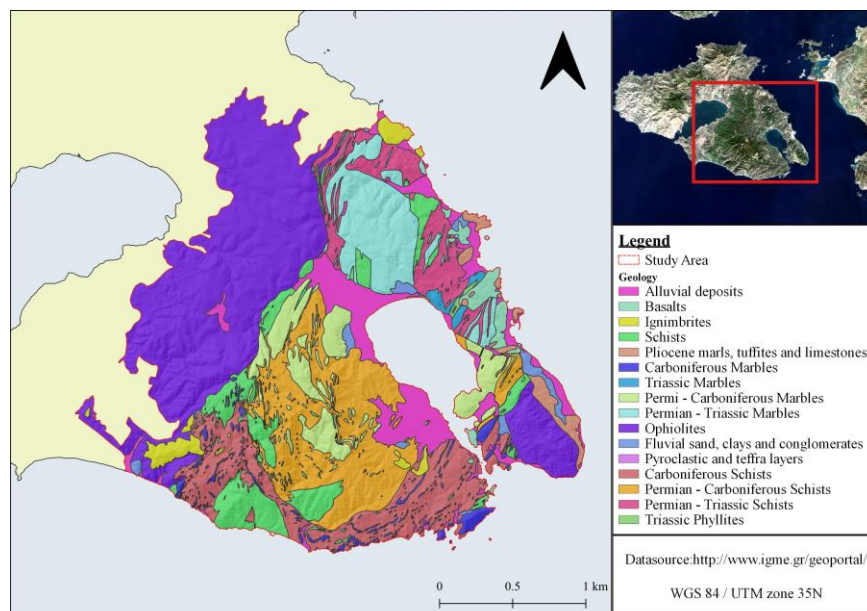


Figure 1. Geological map of the Study area

Solomon and Quiel (2006), developed a "Ground Water Potential Index" depending only on 4 input data as opposed to Krishnamurthy et al. (2000), lithology, lineaments, geomorphology and slope. The thematic layers are weighed up on an empirical basis and the study is more complete as it is also verified with in situ data. Solomon and Queil's GPI is now widely used in many variations such as the GWP by Abdalla (2012).

GPI was used also by Greek researchers (Partsinevelou et al, 2012) and it was applied on the island of Naxos. The index was adjusted to the available dataset for Naxos and the criteria were weighted with the AHP (Analytic Hierarchical Process) which is a statistical method developed by Saaty (1980). AHP compares the layers per pair of clusters and nodes and a scoreboard is constructed, with the weights, divided by their sum for all criteria.

2.2 Aim and purpose

The purpose of this work was to develop a methodology for identifying potential groundwater zones using remote sensing data and GIS. The proposed methodology is based on the empirical GPI (Modified Groundwater Potential Index) and the criteria were adjusted to the characteristics of the study area. The layers were weighed by using the Analytic Network Process (ANP), which is a generalization of the AHP and which is taking into account the dependence between the hierarchies of the different layers (Saaty, 1996; 2005).

The aim was to highlight the potential of remote sensing in the assessment of groundwater areas through the processing of satellite images and the development of a modern and user-friendly methodology for identifying these areas. The designed methodology was derived from the parallel study and research of all factors affecting the presence of groundwater. It also weighed each criterion based on its hydrogeological significance. The secondary but equally important objective of the paper was to measure as far as possible the validity of the results without in situ measurements.

Finally, another objective was the use of primarily open source software to enable everyone to use the method and to improve it. Open-source software was selected because it is user friendly, it is of a minimal cost and it provides a variety of data processing capabilities. In the field of remote sensing, several "packages" (software and libraries) have been developed with automated processes to enable faster and easier image processing.

3. ANALYSIS

4.1 Dataset

Sentinel - 2A and Sentinel - 2B satellite data were used which are radiometrically corrected according to the ground conditions. The Landsat 8 thermal bands were used to calculate the Soil Moisture Index (SMI). The use of Landsat 8 data, in parallel with that of Sentinel-2, demonstrated the compatibility of the two data sets. In the table below, a detailed list of the images used by satellite is presented.

Table 1. The satellited images used in the paper, sorted by sensor and date

Sensor	SENTINEL- 2		LANDSAT 8
Data source	https://scihub.copernicus.eu		https://earthexplorer.usgs.gov/
Platform	S2A	S2B	--
Date	28/04/2018	23/04/2018	30/04/2018
	07/06/2018	--	--
	17/07/2018	21/08/2018	--
	16/08/2018	31/08/2018	20/08/2018
	--	20/09/2018	21/09/2018
	--	10/10/2018	07/10/2018
	04/11/2018	--	--

In addition to satellite images, the Digital Elevation Model (DEM) and a list of vector data were used. The shapefiles depict anthropogenic structures and physical elements of the study area. They were orthorectified to the coordinate system of the satellite images, in order to have the same spatial reference.

4.2 Methodology

The proposed methodology consists of three main steps, the creation of the thematic layers, the Analytic Network Process (ANP) and, finally, the identification of potential zones by calculating the MGPI. Prior to the above steps, the selected satellite images were processed and clipped by a vector mask to the boundaries of the study area to reduce the amount of data. Also, all the vector data needed for the analysis were converted to raster format.

The processing of Sentinel-2 satellite images included the selection of the desired spectral bands (blue, green, red, NIR and SWIR), the application of the vector mask in the study area and the calculation of the NDVI. For Landsat 8 data, only the thermal bands were selected, and the radiation values were converted to temperature values. Finally, to calculate the SMI, the derived from Landsat temperature was combined with Sentinel's NDVI data, which was resampled to the same spatial resolution as the thermal bands.

Table 2. The formulas used to calculate the NDVI and the Temperature

Sensor	Formula		Constants		
Sentinel	NDVI	$\frac{NIR - RED}{NIR + RED}$	--		
Landsat 8	DN to radians (L)	$M_L * Q_{cat} + A_L$	M_L	0,0003342	
			Q_{cat}	TIRS	
			A_L	0,10000	
	Radians to Temperature	$\frac{K_2}{\left(\ln \frac{K_1}{L}\right) + 1}$		B10	B11
			K_1	774.89	1321.08
K_2			480.89	1201.14	

Source: <https://landsat.usgs.gov/using-usgs-landsat-8-product>

The creation of the thematic layers needed for the MGPI was different for each layer. The layers used as input were the elevation and slope, the porosity, the lineaments, the drainage density, the land cover and the thickness of vegetation. Having collected the necessary data, each thematic layer was categorized into 4 classes, low (1), moderate (2), good (3) and very good (4) based on their water permeability. Each criterion was then weighed up using the ANP, as proposed by Saaty (1996). Finally, a weighted map was created by calculating the MGPI index, which is multiplied by the % as it represents the groundwater prospect.

3.2.1 Creation of each thematic layer

3.2.1.1 Elevation and slope

Having observed the DEM's values, the highest is the peak of Olympus at 968 meters. The range is 0 - 968, with 0 being the coastline. The values have an irregular change between high and low values, resulting in several slopes on the ground, which control the movement of water to the lower altitude (Abdalla, 2012). This has as a result that low altitude areas are more likely to collect groundwater and thus have a higher water permeability than the others. The four categories are 0 - 242 (Very good: 4), 243 - 484 (Good: 3), 485 - 726 (Moderate: 2) and 727 - 968 (Low: 1).

The slope layer was produced from the DEM. Slope significantly affects the presence, movement or drainage and recharging of groundwater on one surface (Srinivasa Rao & Jugran, 2003; Abdalla, 2012). Therefore, slope could be considered as one of the most important factors for the presence and flow of groundwater (Mondal, 2016). The surface run-off is usually slow in areas with mild slope, allowing for faster filtration of water and the recharge of the aquifer. In contrast, in the steep slope areas, the drainage is greater and faster and the rainwater cannot penetrate and recharge the local aquifers (Abdalla, 2012; Partsinevelou et al, 2016). Therefore, the probability that there is a groundwater zone in a mildly inclined area is greater than in one with a higher inclination. The slope is divided to four classes and the range of each class in degrees is 0 – 16.18 (Very Good: 4), 16.19 – 32.35 (Good: 3), 32.36 – 48.53 (Moderate: 2) and 48.54 – 64.7 (Low: 1).

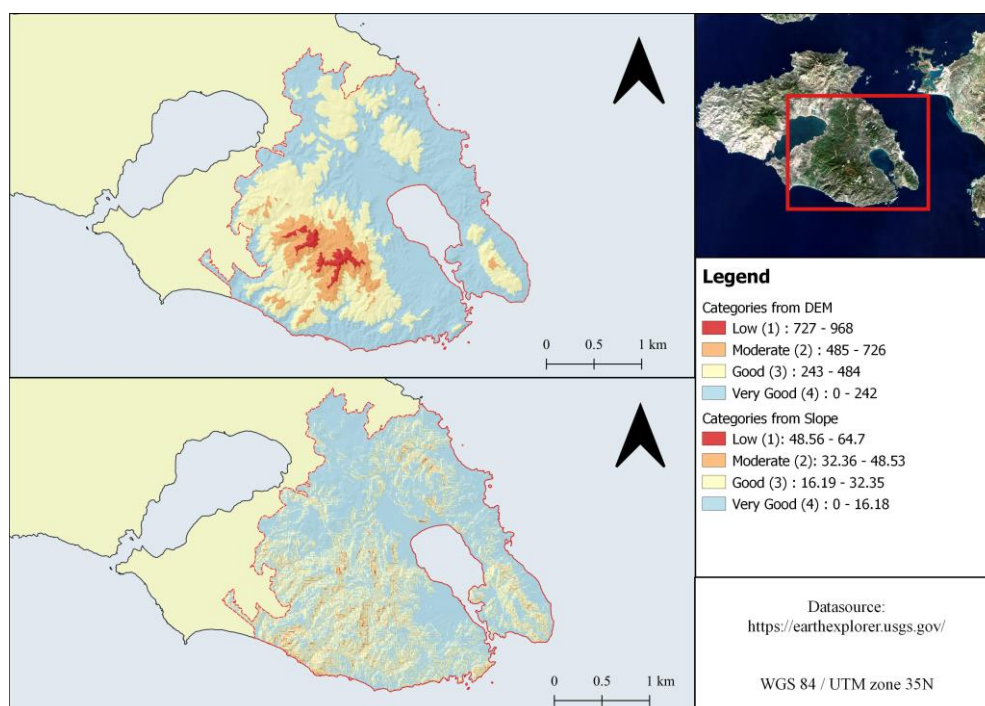


Figure 2. Map of the classification of the elevation values derived from the DEM (above) and the Slope (below) layers

3.2.1.2 Land cover and vegetation

To create the land cover layer, the image was classified using Object Based Image Analysis (OBIA). This method differs from the other spectral image classification methods because the necessary information/training areas are derived from primitive objects created by the segmentation process. These objects are polygons of different layers based on their texture or color. For the classification, the image used was the one from 4/11/2018 (Sentinel 2) and was classified in 5 categories based on Corine Land Cover Level 2 data for 2012. Those 5 categories were urban areas, sclerophyllous vegetation, forests, crops and olive groves.

Firstly, samples, from each category were defined and then the primitive objects were classified with nearest neighbor. After completing the classification an accuracy/assessment check was completed using training areas from the image (TTA

mask). The results of the accuracy/assessment check are statistical measurers for each class, the overall accuracy of the classification and the K- index of accuracy (KIA). The overall accuracy was 0.9166 and the KIA 0.8912. According to these, the classification was 90% close to reality and the result was accepted.

Table 3. The statistical measures for each class after completing the accuracy/assessment check

Categories	Stats				
	Objects	Mean	Standard deviation	Max	Min
Urban Areas	178	0.01	0.03	1.62	0.18
Forest	65	0.0001	0.0001	1.37	0.0008
Crops	78	0.0001	8.749	8.34	0.0002
Sclerophyllous Vegetation	46	2.23	1.92	1.78	7.89
Olive Groves	11	9.60	8.22	1.25	0.0002

To categorize the different land cover classes according to their water permeability, each class was studied separately. The class with the less water permeability is the urban area because the existence of buildings restricts the existence of vegetation, resulting in greater erosion in the soil and no water being stored in it. Also, low water permeability has the crops and the olive groves classes, this is because most of the crops are affected by lakes and groundwater, resulting in non-smooth surface drainage and underground drainage, so no more water is penetrated into the soil than the necessary for the growing crops.

Natural vegetation like forest and areas covered with sclerophyllous vegetation, has the highest water permeability. Groundwater reserves are regularly renewed on the ground, but the vegetation's ability to use or evaporate the water from the ground also determines the speed of its renewal. The deep root systems of many indigenous trees can use more water than other types of vegetation and reduce the stock of water in the soil. Thus, forests were given lower marks than the sclerophyllous vegetation, because the larger and denser the trees and their foliage, the more water they consume.

Table 4. The land cover categories

Land Cover Classes	Category
Urban Areas	1
Forest	3
Sclerophyllous Vegetation	4
Olive Groves	2
Crops	2

As mentioned above, vegetation can affect the movement of water underground. Vegetation is an equally important factor affecting the existence of groundwater because the water flow transfers nutrients to the soil and can change the type and amount of vegetation in an area. So, the denser the vegetation, the greater the water permeability. The average of the NDVI index was categorized into four classes, in terms of the density of vegetation, considering the land cover classification.

Table 5. Water permeability categories based on the NDVI

NDVI Value	Vegetation Thickness	Category
-0.8 - 0	Low	1
0.1 – 0.3	Moderate	2
0.31 – 0.61	High	3
0.62 – 0.92	Very High	4

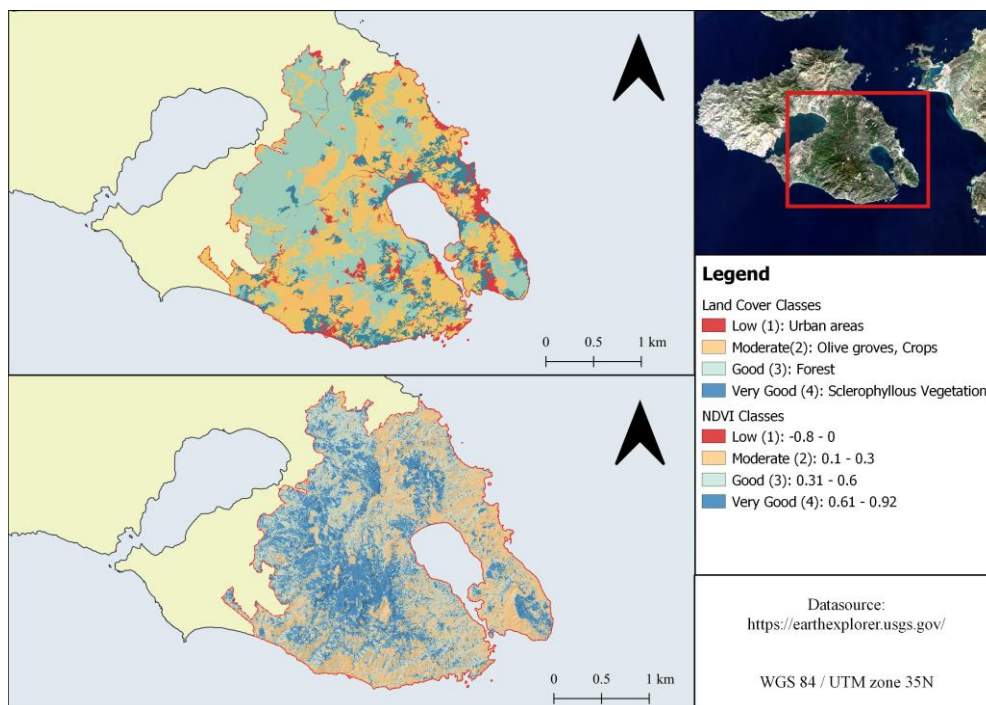


Figure 3. Map of the classification of Landcover (above) and the NDVI (below)

3.2.1.3 Rock porosity

Geology of the study area consists mainly of metamorphic and sedimentary rocks, and rarely of some ophiolites. Generally, there are many loose sediments and deposits with high porosity in the area. The porosity in a rock is defined as the ratio of the volume of gaps to the total volume of the rock and is expressed in percentage (Papanikolaou & Sideris, 2013).

The higher the value of porosity, the greater the gaps inside the rock, so the greater their water permeability. However, the high porosity in a rock does not mean high water permeability as it depends on the size of the voids inside the rock. Rocks with low porosity values have small water permeability and do not allow water to circulate inside them. A bibliographic (Mountrakis 2010; Papanikolaou & Sideris 2013; Partsinevelou et al, 2010) and empirical research was conducted to sort each major rock category by its porosity.

Table 6. Rock Porosity by type of rock

Type of rock	Porosity	Category
Basalts, Phyllites, Marbles	Low	1
Ignimbrites, Ophiolites, Schists	Moderate	2
Marls, Tuffites, Limestones	High	3

Alluvial deposits, Fluvial Sand, Conglomerate, Clays	Very High	4
--	-----------	---

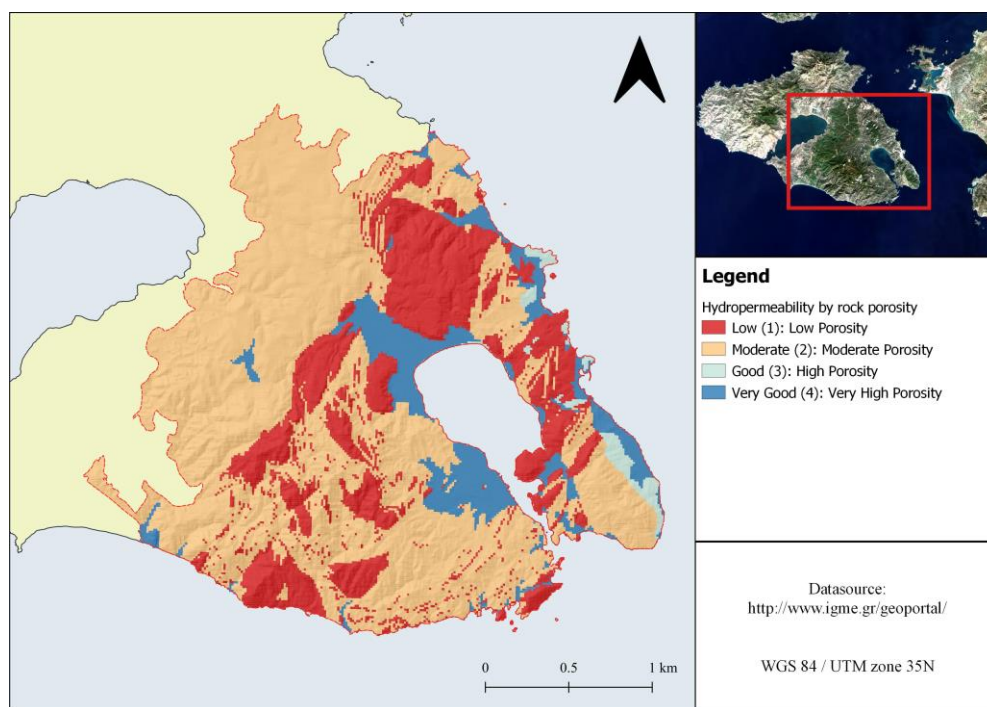


Figure 5. Map of the porosity by type of rock

3.2.1.4 Lineaments

Lesvos is located south of the north end of the Anatolian Fault and features a complex fault pattern (Soulakellis et al, 2006). A fault can be observed as a lineament in a satellite image. Lineaments are linear features in a landscape that are an expression of an underlying geological structure. Locating and mapping lineaments is a particularly important issue in hydrogeological research as the existence and circulation of groundwater in low-porosity rock regions depends on their density (Abdala, 2012; Partisinelou et al, 2016).

There are a number of methods for detecting lineaments through remotely sensed data, but in this paper a 3-step method proposed by Marghany & Hashim (2010) was applied. The first step is the equalization of the image histogram, the second is the application of the Canny edge enhancement filter, and finally, it is the digitization of the newfound lineaments. The 3-step method was tested on a Sentinel 2 image because of its higher resolution. To verify the results, already mapped lineaments from Soulakellis et al (2006) and Hecht (1972) were used. The results can be seen in figure 6.

To finalize the results, a spatial density map was created. Spatial density expresses how many objects (linear and dot) are in the given space. The density was divided into 4 categories, low, medium, large, and very large. Having defined the categories, the water permeability scoring is done. The areas with high density are the ones with the highest water permeability as the fracture in the soil allows easier circulation of water in the soil, while in the areas of low density, the water permeability is low. The lineament density is categorized to four classes, the values for each class in m^2 are low density (0 –

0.46, Low: 1), moderate density (0.47 – 0.92, Moderate: 2), high density (0.93 – 1.38, Good: 3) and very high density (1.39 – 1.84, Very good: 4).

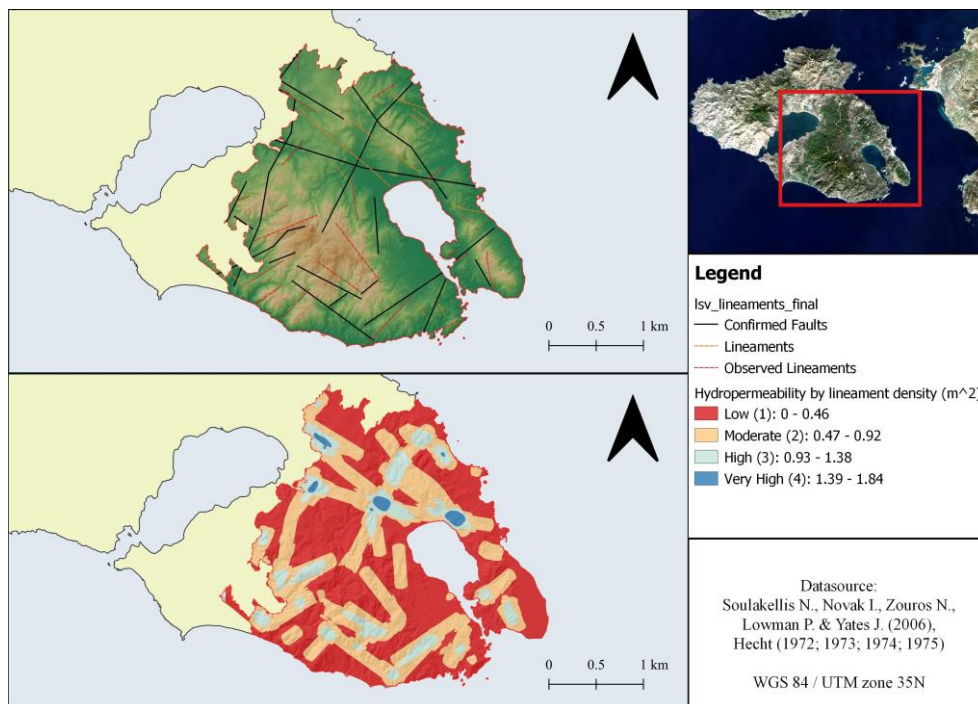


Figure 6. Map of the lineaments and their density

3.2.1.5 Drainage Density

The drainage density indicates the proximity of the distance between the water flows to the ground (Partsinevelou et al, 2010) and when its value is high, the water runoff is also high. To calculate the drainage density, the DEM was used, which provides basic spatial reference and the ability to create geomorphological models (Çanapuram et al, 2009 ; Mokarram & Sathyamoorthy, 2015 ; Bezinska & Stoyanov, 2019), so the following files were produced the drainage direction and the flow accumulation.

The procedure for calculating the drainage density included five steps, the conversion of the created layers to vector, the check and union of the flow accumulation lines, the demarcation of the basin layer to individual layers, the calculation of the length of the flow accumulation lines in each basin in km and the area of each basin in km², finally the application of the mathematical formula of the drainage density. The density was classified to four categories low density (0 – 1, Very good: 4), moderate density (1.01 – 2.01, Good: 3), high density (2.02 – 3.02, Moderate: 2) and very high density (3.03 – 4.03, Low: 1).

$$D. D. = \frac{SUM(L)}{A}, \text{ L is the length of the flow and A is the area of the catchment.}$$

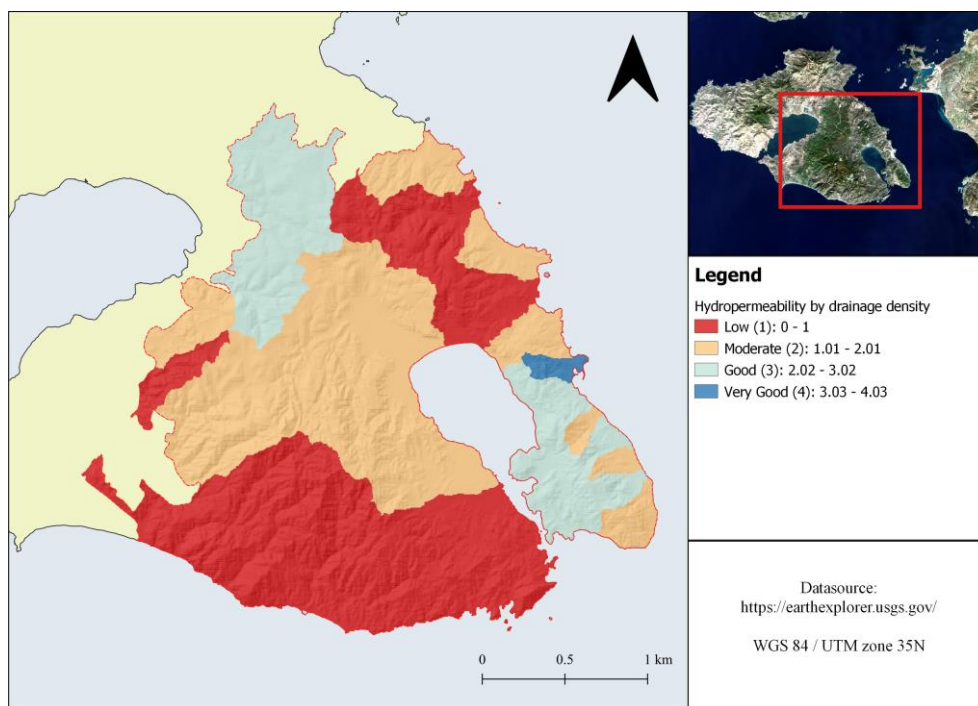


Figure 7. Map of the drainage density

3.2.2 Analytic Network Process

In order to delineate the potential groundwater zones, the criteria were combined with the implementation of the Analytic Network Process. ANP was created by Saaty (1996) and is a generalization of the Analytic Hierarchy Process (Saaty, 1980). Most decision problems cannot be hierarchically structured because there is interdependence between elements. Therefore, ANP examines this dependency and its structure is reminiscent of a network rather than a hierarchy, as in AHP, with nodes and loops linking the criteria together (Saaty, 1996). Also, includes clusters, which each is linked to the elements of another cluster or its clusters where it belongs (Nekhay et al, 2009). ANP consists of 4 steps, which are analyzed below.

In the first step, the clusters and the nodes are defined and are compared in pairs according to Saaty's "expert scale", ranging from 1 to 9, where 1 indicates that the elements are of equal importance, while 9 indicates that one element is superior to the other. Having defined clusters and nodes (Figure 8), the relationships between them are investigated. The result of cluster comparison is the cluster matrix, which illustrates the relative importance between clusters (Saaty, 1996). One cluster affects another when connected and when at least one node is associated with one node of the other. To validate the consistency of the results the confidence ratio, which should be less than 0.1, is used.

Table 7. The layers sorted by the most to the least important and their comparison according to Saaty's expert's scale

Layers	Slope	Elevation	Rock Porosity	Lineament Density	Drainage Density	Vegetation Thickness	Land cover
Slope	1	2	3	5	6	7	8
Elevation	1/2	1	2	4	5	6	7

Rock Porosity	1/3	1/2	1	3	4	5	6
Lineament Density	1/5	1/4	1/3	1	2	4	6
Drainage Density	1/6	1/5	1/4	1/4	1	4	6
Vegetation Thickness	1/7	1/6	1/5	1/4	1/4	1	2
Land cover	1/8	1/7	1/6	1/6	1/6	1/2	1
Confidence Ratio	0,06150	0,07320	0,08338	0,07873	0,07263	0,07845	0,08336

The second step is to create the supermatrix table, which contains all the data and the corresponding weights. This table is constructed from the priorities that result from different pairwise comparisons (Saaty, 2001). Each column deals with a node and its effect on an element to the left of the matrix on an element at its top, with reference to a particular cluster.

The third step involves arranging the clusters from the most important to the least important. This rating takes into account the cluster matrix table, created in the second step. The result is the weighted matrix, which mathematically captures the importance of each cluster (Saaty, 2001) and of each node within it. To “weight” the clusters and make it obvious which is the most important, multiply the cluster matrix table by the total matrix table. This multiplication results in the weighted supermatrix.

The fourth and final step of the analysis is the limit matrix, which defines the final priorities among the nodes (Saaty, 2001). This table results from the multiplication of the weighted matrix table by itself, as many times as each row of the table reaches the same value (Agarwal et al, 2013). The basic principle of the limit matrix table is that in addition to the same result in each row, the sum of its columns is the same (Saaty, 2001; Nekhay et al, 2009). Having acquired all the necessary tables in the previous steps, they are normalized and synthesized to calculate the weight for each class.

Table 8. Clusters and nodes with their respective weight factor

Clusters	Nodes	Category	Weight
Elevation	0 – 242	4	0.2544
	243 – 484	3	
	483 – 726	2	
	727 – 968	1	
Slope	0 – 16,18	4	0.2947
	16,19 – 32,35	3	
	32,36 – 48,53	2	
	48,54 – 64,7	1	
Landcover	Urban area	1	0.0279
	Crops	2	
	Olive groves	2	
	Forest	3	
	Sclerophyllous Vegetation	4	
Rock Porosity	Low	1	0.1813
	Moderate	2	
	High	3	
	Very High	4	

Lineament Density	Low (0 – 0.46)	1	0.113
	Moderate (0.47 – 0.92)	2	
	High (0.93 – 1.38)	3	
	Very High (1.39 – 1.84)	4	
Drainage Density	Low (0 – 1)	4	0.0878
	Moderate (1.01 – 2.01)	3	
	High (2.02 – 3.02)	2	
	Very High (3.03 – 4.03)	1	
Vegetation Thickness	Low (-0.8 – 0)	1	0.0404
	Moderate (0.1 – 0.3)	2	
	High (0.31 – 0.61)	3	
	Very High (0.62 – 0.92)	4	

3.2.3 Modified Ground Water Potential Index (MGPI)

MGPI's main feature is that its result is a dimensionless quantity that serves to find potential groundwater zones in an area (Murasingh et al, 2018). This amount is usually perceived as a percentage, or its lower values reflect a lower probability of having a groundwater zone. The index is calculated by multiplying each parameter (P_i) by the corresponding weight (W_j) and finally summing the resulting products. The result of the index was classified into 4 classes based on the probability of water in the soil pores. These classes are low (1), moderate (2), good (3) and very good (4). The calculation was made in a GIS environment, using the layers in raster format and the weights resulting from the ANP.

$$MGPI = \sum (P_i * W_j)$$

4. RESULTS AND VALIDATION

The final result is a thematic map which illustrates the result of the MGPI equation. The most likely to have an underground aquifer is the area in the SW of the study area, the wider forest area of Agiassos. This area has high altitude, dense vegetation, moderate drainage and large porosity in the rocks high altitude areas, dense vegetation, moderate drainage and high rock porosity. Also, the Amali peninsula has low drainage and therefore low runoff, steep slopes, high dense vegetation but low porosity. Land cover is forestry (probably the Haramida forest), so tree roots create gaps in the soil, thus facilitating water filtration, regardless of the value of rock porosity.

The area between Mystegna and Saint Raphael was categorized as having a moderate probability of groundwater potential. Its main features are dense vegetation, moderate porosity, low slope, high line density, and not particularly high altitude (340 meters) than other areas, but it has high drainage density. The area of Plomari is characterized with moderate probability of groundwater potential. The area, however, is characterized by high water density and its rocks have low porosity. The main land cover is olive groves and vegetation is particularly dense. The altitude is high and the slopes values, which is the most important factor, are not large. It is also observed that the points with little or no probability of being water-permeable are along the coastline in low altitude areas with high drainage density, such as the Evergetula River Basin. This is to be expected,

since the circulation of groundwater is directly dependent on the topography of an area and the denser the drainage the greater the runoff, allowing the water to escape directly into the sea.

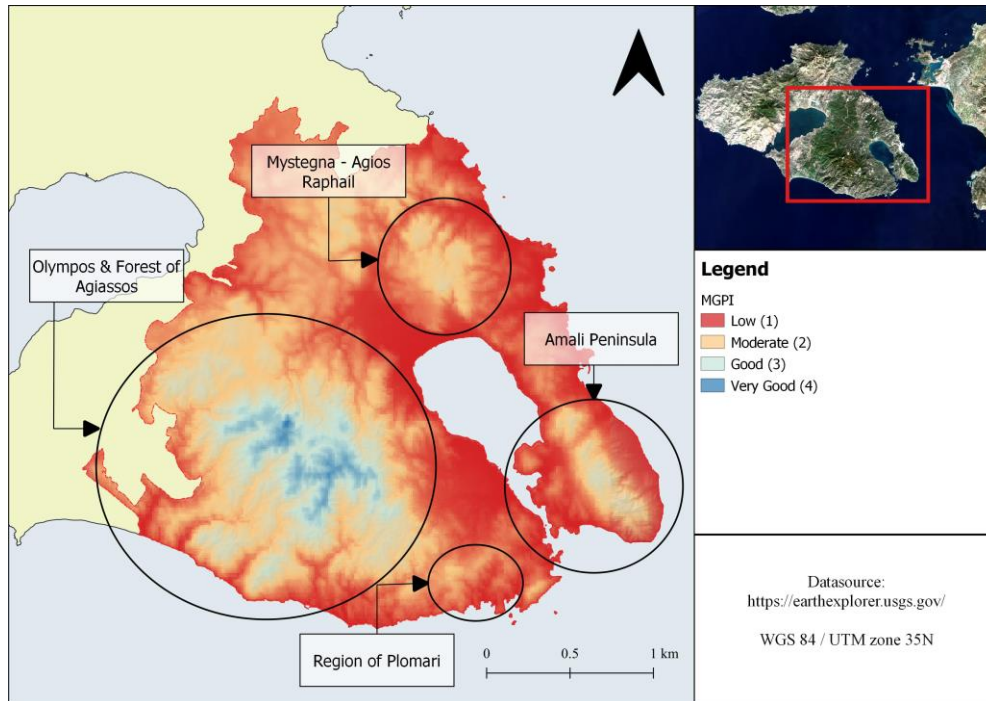


Figure 8. The result of MGPI

To validate the results, data from the confirmed groundwater zones, as listed in the Lesvos Water Supply Master Plan (DEYAL, 2017) and the SMI were used. There are 8 groundwater zones in the study area, as seen in figure 9. Based on the results obtained when calculating the MGPI, the region is characterized by a moderate probability, but in the vicinity of that of Sedounda – Plomari complex the probability increases (good). In the Sedounta - Plomari complex it is also most likely to locate groundwater.

The Larso's complex is of moderate probability because the area is mainly covered by marbles, which are particularly vulnerable to water solubility. The area where the MGPI is low is in the complex Gera's bay. The result of the index is not realistic in this case, since in the area there is a large, confirmed amount of groundwater. This is probably due to the way the criteria are scored and weighted, as well as the fact that the drillings which confirm the existence of water are point-based, with the index taking into account a pixel grid which contains more than one point.

More generally, in all cases reported, the MGPI has calculated probability of existence by analyzing various thematic levels that affect the existence of the underground aquifer. In addition, the moisture index SMI is used, which indicates the amount of water available in the soil and is considered one of the most "realistic moisture indicators" (Hogg et al., 2013). Soil moisture is an important factor for the existence of groundwater, as part of the water stored in the soil pores is used to fill the surface moisture (Kumar & Seethapathi, 2002).

The calculation of the SMI is directly related to the NDVI and the temperature and the changes between them. The model is computed using empirical parameters derived from

the scatter plot of pixel values in two-dimensional temperature space (T_s) and NDVI (Sridhar et al, 2008). The SMI calculation model includes the empirical determination of the two lines delineating these two ends (Meng et al, 2008) and its range is $[-1,1]$, where 0 is dry land and 1 is wet. SMI was calculated for the 4 Landsat images, with a maximum of 3 days between images and a minimum of 1 day. To calculate the index a pre-made python script available online was used, altered in certain parts.

Table 9. The formulas used to calculate the SMI

Dry Edge	$T_{S_{max}} = (a_1 * NDVI) + b_1$
Wet edge	$T_{S_{min}} = (a_2 * NDVI) + b_2$
SMI	$SMI = \frac{T_{S_{max}} - T_s}{T_{S_{max}} - T_{S_{min}}}$

The area that has the highest moisture values is the complex of Gera, which is also the first zone to exploit its reserves. The results of the SMI appear to be more representative than those of the MGPI. This is due to the fact that the SMI accepts only two factors for its calculation, vegetation and temperature, without being weighted. Also, the calculations are made per pixel, so they are points and refer to the space that each pixel occupies. SMI also has high values in the southern part of the Amali peninsula (Mytilene zone) but also in the boundaries between the ophiolites' zone and the Larssos complex.

Apart from these areas, it is observed that high SMI values are also present in areas with high NDVI values. Increased soil moisture favors vegetation and especially dense vegetation, where it requires large amounts of water to maintain it. Consequently, the high moisture value is directly linked to vegetation and therefore to groundwater, since the dense root system creates fragments within the soil that allow water to pass through.

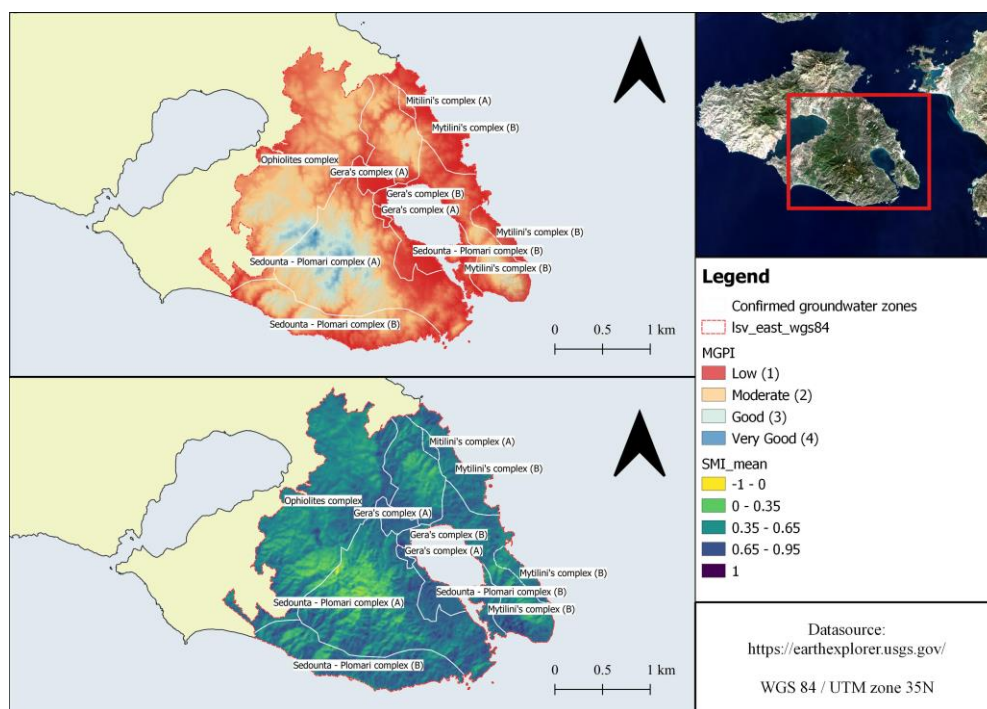


Figure 9. The results of the indices (MGPI above and SMI below) in comparison with the confirmed groundwater zones

5. CONCLUSIONS

The ability of soil to store water provides humans with an alternative source of water, since surface water is insufficient to meet the needs of the growing population. This work identified potentially groundwater supply areas using remote sensing. The approach to the scientific question concerns whether the various environmental and topographical factors influence the existence of an aquifer. The main processing of the satellite data and the rest of the data was aimed at producing certain thematic levels, such as vegetation and soil slopes, which are directly related to groundwater.

By studying and weighting these criteria, the MGPI empirical index was calculated, which does not accept specific input data, but the researcher selects them based on their needs and data availability. In this case, the input data were selected based on the characteristics of Eastern Lesvos and this could be considered as the greatest advantage of the method. The layers were weighted using the ANP multivariate statistical method. The positive aspect of ANP is that it takes into considerations the interactions that occur even in nature and does not ignore external factors. The result is a spatial distribution of the probability of the existence of an underground aquifer in a wider area.

Based on the result, a greater probability of 83.86 % was found in the Olympus area and in the Agiassos forest, due to the fact that the geological background is karstic and in combination with the large root system of the forest, the water flows more easily. The areas with lower water permeability are those along the coastline, which due to high runoff do not permit collection of water in the soil pores.

The results of the MGPI index are at pixel level and are not point-based, so they need to be verified by ground measurements. Therefore, to verify the result, it is not enough to just check the data for the already confirmed zones or calculate the SMI. It is necessary to conduct in situ measurements at various points within the areas identified in order to have a more complete picture and to evaluate if the result is reliable or not.

It is recommended for further analysis and study, to obtain field measurements and to combine with satellite data, not only from Sentinel but also other sensors. It is also important to make comparisons over time to determine whether the zones change. It is also considered interesting to correlate the results with rainfall data, which is the main source of groundwater potential renewal.

REFERENCES

- Abdalla F. (2012), Mapping of groundwater prospective zones using remote sensing and GIS techniques: A case study from Central Eastern Desert, Egypt, *Journal of African Earth Sciences*, 70, 8–17
- Agarwal E., Agarwal R., Garg R. & Garg P. (2013), Delineation of groundwater potential zone: An AHP / ANP approach, *J. Earth Syst. Sci.*, 122, 3, 887 - 898
- Bezinska G. & Stoyanov K. (2019), Modelling and hydro-morphometric analysis of sum-watershed. A case study of Mesta river southwestern Bulgaria, *European Journal of Geography*, 10, 2, 77-88

- Ganapuram S., Kumar V.G.T., Krishna M.I.V, Kahya E. & Demirel C.M. (2009), Mapping of groundwater potential zones in the Musi Basin using remote sensing data and GIS, *Advances in Engineering Software*, 40, 506 - 518
- Hecht J. (1972), Geological Map of Lesvos Island (Plomari – Mytilene) Sheet, 1:50 000, Greek Institute of Geology and Mineral Exploration - IGME.
- Hogg E. H., Barr A. G., Black T. H., (2013), A simple soil moisture index for representing multi-year drought impacts on aspen productivity in the western Canadian interior, *Agricultural and Forest Meteorology*, 178-179, 173-182
- Katsikatsos G., Mataragas D., Migiros G. & Triantaphyllis E. (1982), Geological study of Lesvos Island, I.G.M.E (internal report), Athens.
- Krishnamurthy J., Mani A., Jayaraman V. & Manivel M. (2000), Groundwater resources development in hard rock terrain – an approach using remote sensing and GIS techniques, *International Journal of Applied Earth Observation and Geoinformation*, 2, 204–215
- Kumar, C. P. & Seethapathi P. V. (2002), Assessment of Natural Groundwater Recharge in Upper Ganga Canal Command Area, *Journal of Applied Hydrology*, Association of Hydrologists of India, Vol. XV, 4, 13-20
- Marghany M. & Hashim M. (2010), Lineament mapping using multispectral remote sensing satellite data, *International Journal of the Physical Sciences*, 5, 10, 1501-1507
- Meng L., Li J., Chen Z., Xie W., Chen D., Duan H., (2008), The calculation of TVDI based on the composite time of pixel and drought analysis, *The International Archives of the Photogrammetry, Remote Sensing and Spatial Information Sciences*, 38, 518-524
- Mokarram M. & Sathyamoorthy D. (2015), Morphometric Analysis of Hydrological behavior of North Fars watershed, Iran, *European Journal of Geography*, 6, 4, 88-106
- Mondal S., (2016), Research progress in landslide potentiality assessment: A case study of the Shiukhola watershed, Darjiling Himalaya, *European Journal of Geography*, 7, 2, 21-47
- Mountrakis D. (2010), Γεωλογία και Γεωτεκτονική εξέλιξη της Ελλάδας, Εκδόσεις University Studio Press, Θεσσαλονίκη
- Murasingh S., Jha R. & Adamala S. (2018), Geospatial technique for delineation of groundwater potential zones in mine and dense forest area using weighted index overlay technique, *Groundwater for Sustainable Development*, 7, 387 - 399
- Nekhay O., Arriaza M. & Boerboom L. (2009), Evaluation of soil erosion risk using the Analytic Network Process and GIS: A case study from Spanish mountain olive plantations, *Journal of Environmental Management*, 90, 3091 - 3104

- Papanikolaou D. & Sideris C. (2013), Γεωλογία: Η επιστήμη της Γης, 6η έκδοση, Εκδόσεις Πατάκη, Αθήνα
- Partsiouvelou A. – S., Eurenoglou L. & Stournaras G. (2016), Simulation of the groundwater flow in hard rock hydrogeological environments. Application in Naxos Island, Greece, *International Journal of Geology*, 10, 11 – 17
- Rao Srinivasa Y., & Jugran D. (2003), Delineation of groundwater potential zones and zones of groundwater quality suitable for domestic purposes using remote sensing and GIS, *Hydrological Sciences*, 48, 5, 821 - 833
- Saaty T.-L. (1980), *The Analytic Hierarchy Process: Planning, Priority Setting, Resource Allocation*, McGraw - Hill, New York
- Saaty T.-L. (1996), *Decision Making with dependence and feedback: The Analytic Network Process*, RWS Publications, Pittsburg, USA
- Saaty T.-L. (2001), *Decision Making with dependence and feedback: The Analytic Network Process*, Second Ed., RWS Publications, Pittsburg, USA
- Sridhar V., Hubbard K.G., You J., Hunt E.D. (2008), Development of the soil moisture index to quantify agricultural drought and its “user friendliness” in severity-area-duration assessment, *Journal of Hydrometeorology*, 9, 660–676
- Solomon S. & Quiel F. (2006), Groundwater study using remote sensing and geographic information systems (GIS) in the central highlands of Eritrea, *Hydrogeology Journal*, 14, 1029 -1041
- Soulakellis N., Novak I., Zouros N., Lowman P. & Yates J. (2006), Fusing Landsat-5/TM Imagery and Shaded Relief Maps in Tectonic and Geomorphic Mapping: Lesvos Island, Greece, *Photogrammetric Engineering & Remote Sensing*, Vol.72, 6, 693-700
- Srinivasa Rao Y. & Jugran D.K. (2003), Delineation of groundwater potential zones and zones of groundwater quality suitable for domestic purposes using remote sensing and GIS, *Hydrological Sciences – Journal des Sciences Hydrologiques*, 48, 5, 821 – 833